Beni-Suef University Journal of Basic and Applied Sciences

RESEARCH

Open Access

Assessment of nano-iron particles impact on the reproductive health of female Wistar rats

Menna-Tullah Magdy[1], Abd EL-Wahab A EL-Ghareeb[2], Fawzy A Attaby[3] and Heba A Abd El-Rahman[2*]

Abstract

Background: Iron oxide nanoparticles, especially nano-magnetite, are promising candidates for use in a variety of applications. The present study aimed to investigate the effect of nano-magnetite on the reproductive health of female Wistar rats. Twenty-one adult female rats were divided into three groups: Group 1 served as the control group, Group 2 received a low dose of 5 mg/kg of nano-magnetite, and Group 3 received a high dose of 10 mg/kg of nano-magnetite. For 30 days, rats were intraperitoneally injected three times per week.

The main findings: Revealed that nano-magnetite did not induce a change in body weight or absolute as well as relative reproductive organs weight. Nano-magnetite nanoparticles influenced the reproductive serum hormone levels as well as imbalanced the ovarian and uterine malondialdehyde and total antioxidant activity. After nano-magnetite nanoparticle injection, the histopathological examination revealed apoptosis of granulosa cells of various types of follicles, degenerated corpora lutea, congested blood vessels, and uterine epithelial cells of uterine tissue showed a high level of apoptosis and inflammation. Immunohistochemistry studies demonstrated a significant increase in activated caspase-3 following nano-magnetite injection, indicating an increase in cell apoptosis.

Conclusion: This study demonstrated the negative effect of magnetite nanoparticle on reproductive health and increased the likelihood of infertility.

Keywords: Magnetite nanoparticles, Female Wistar rat, Reproductive health, Histopathology, Hormones

1 Background

Nanomaterials (NMs) contain 50% or more nanoparticles (NPs) with more than one external dimension in the 1–100 nm size range [1]. Due to their small size, NPs have been widely utilized in many fields [2]. The wide applications of NMs have highlighted their significance as well as biological effects [3].

Magnetite (Fe_3O_4), also known as black iron oxide, magnetic iron ore, and loadstone, is one of the iron oxides known as the oldest magnetic material. Magnetite mineral crystallized with Fe_3O_4 chemical formula in spinel structures has the strongest magnetism among other iron oxide phases [4]. The magnetite nanoparticles have a greater chance of being efficiently integrated into environmental contaminant elimination and cell separation, magnetically guided drug delivery, magnetocytolysis, sealing agents (liquid O-rings), dampening and cooling mechanisms in loudspeakers, and contrast agents for magnetic resonance imaging (MRI) [5].

Previous research has revealed that certain types of NPs can pass through specific biological barriers and have a negative impact on vital organs, like the brain, liver, and kidneys. Furthermore, a study suggested that the accumulation of silver NPs within the main organs (most significantly in the liver, lungs, and spleen) occurs after intravenous injections and then gradually decreases [6]. Additionally, it has been shown that a single intravenous injection of gold NPs may cause a long-term accumulation in the liver and spleen [7]. The gradual accumulation of NPs in kidneys, blood, and testis and their gradual reduction from urine, feces, and lungs

*Correspondence: ha793481@gmail.com; hebaabdelrahmanan15@cu.edu.eg

[2] Department of Zoology, Faculty of Science, Cairo University, Giza, Egypt
Full list of author information is available at the end of the article

indicate the inefficient clearance of NPs from the urine and feces and undergoing redistribution. Regardless of the exposure route, animal model, or physicochemical properties of the NPs used, the liver and kidneys are the most common accumulation organs [8].

NPs can also penetrate some biological membranes and accumulate in reproductive organs. Kim et al. [9] demonstrated that 50 nm magnetic NPs could penetrate the mouse BTB (blood–testis barrier) and be deposited in the testes and other reproductive organs, causing further damage to these organs. Titanium dioxide (TiO_2) NPs can accumulate in the cytoplasm and nuclei of ovarian cells and induce apoptosis. A previous report revealed that after exposure to TiO_2 NPs, the ultrastructure of the mitochondria and nuclei of ovarian cells was impaired. Mitochondrial swelling and rupture, nuclear chromatin condensation, and nuclear membrane irregularity were observed [10]. Another study indicated that exposure to nickel NPs resulted in ovarian lymphocytosis, luteal cell increase, and cavitation increased eosinophils and inflammatory cell infiltration in rat ovarian tissues [11]. Intact NPs were detected in hen ovarian tissues after treatment with ZnO NPs, and treatment significantly decreased the egg yolk lipid content [12]. All three kinds of NPs have the potential to deposit in ovarian cells and further damage these cells at the molecular and genetic levels; these injuries may have a direct effect on fertility. The reproductive toxicity of nanomaterials has recently been brought to light. They can pass across the blood–testis, placental, and epithelial barriers that protect reproductive tissues and accumulate in reproductive organs. As a result, NPs can enter the female reproductive system and cause damage to the female reproductive organs and cells, resulting in reduced fertility and embryonic development [3].

Reproductive health is a condition of complete physical, psychological, and social well-being, not just the absence of disease or illness, in all elements of the reproductive system and its roles and processes. If the reproductive health is malfunctioning, this will affect the capability of women to reproduce, which eventually leads in late cases to infertility. Infertility is defined as a couple's inability to achieve pregnancy in an average of 1 year or 6 months despite adequate, regular (3–4 times per week) unprotected sexual intercourse [13]. Infertility can be caused by a fundamental medical disorder that may damage the fallopian tubes, intervene with ovulation, or cause hormonal problems [14].

A study investigated the ION effects on reproduction and offspring in mice treated with DMSA (dimercaptosuccinic acid)-coated magnetite nanoparticles, which demonstrated that even though there were no negative impacts on pregnancy or fetal growth, there was a considerable reduction in offspring growth and maturation after delivery, as well as nearly 70% death before puberty. Furthermore, male progeny had lower numbers of spermatogonia, spermatocytes, spermatids, and mature sperms, implying that ION exposure may impair placental and fetal mouse development [15]. The increased production and use of ION will undoubtedly increase the risk of exposure for both people and the environment. As a result, it is critical to assess the potential health and environmental effects of ION on humans, non-human biota, and ecosystems. Until recently, most studies on the potential effect or toxicity of ION focused on mammals (such as mice and rats) and/or various cell lines [16]. However, only a few studies have looked into the reproductive toxicity of ION to date, mainly in the female reproductive system. To our knowledge, no previous research has investigated the effect of magnetite nanoparticles on the reproductive health of adult female Wistar rats. Therefore, this study aims to investigate the effect of magnetite nanoparticles on the female rat reproductive system after a 4-week intraperitoneal injection.

2 Methods

2.1 Chemicals

Magnetite nanoparticle (n Fe_3O_4) with a published particle size of > 50 nm was purchased from the Nano Gate company (Egypt). The nanoparticles were supplied as a black powder with a specific surface area of 38.57 m^2/g and a purity of 95%

2.1.1 Characterization of nanoparticles

The synthesized Magnetite nanoparticles have been characterized using X-ray diffraction (XRD) (Bruker D8 Discover) in The Center of Nanotechnology, Cairo University, El-Sheikh Zayed branch to prove the existence of a crystalline phase and confirm the degree of crystallinity. Information about the synthesized magnetite nanoparticles was determined using transmission electron microscopy (TEM).

The first part of Fe_3O_4 was used to analyze the microstructure and determine the particle size using transmission electron microscopy (Jeol_Jem_1230 electron microscope).

The morphology of the magnetite particles formed was examined by direct observation via high-resolution transmission electron microscopy for all the collected particles.

The second part was analyzed using X-ray diffraction (Philips X'Pert, CuKa, 40 kV, 30 mA, and $k = 1.54056$ Å) to determine the dried powder's sample phases and average particle size. The magnetization measurements were carried out at room temperature up to a maximum magnetic field (H) of 900 Tesla using VSM homemade.

Cubic single-phase nano-sized Fe_3O_4 powder has been obtained. According to the Debye–Scherrer formula, the crystallite size Dhkl for the sample is given by [17].

2.2 Animals

All the experimental protocols and procedures used in this study were approved by the Institutional Animal Care and Use Committee (IACUC), Faculty of Science (Egypt), Cairo University (CUFS/Comp&Emb/CU/I/F/74/19).

Twenty-one adult female Wistar rats weighing 180–200 g (8 weeks) were purchased from the Faculty of Veterinary Medicine, Cairo University. Animals were housed in hygienic cages with sawdust-covered floors and kept under controlled conditions of heat (22 ± 1 °C), 30–70 percent relative humidity, and a 12-h light/dark cycle.

Animals were allowed to acclimatize for a week before the commencement of treatment. Animals were fed commercial rat chows and had free access to tap water.

2.3 Animal grouping

The animals were randomly assigned into three experimental groups (seven rats per group). The following are animal distribution details:

1. Group 1 (control group): received distilled water.
2. Group 2 (Treated 1): received a low dose of 5 mg/kg.
3. Group 3 (Treated 2): received a high dose of 10 mg/kg

Dosage: Fe_3O_4 NPs powder (500 mg) was dissolved in 50 ml distilled water and dispersed with sonication for 25 min. The doses of 5 and 10 mg/kg bw were chosen based on the findings of a previous study by Ma et al.2012 [18].

2.4 Experimental design

For 30 days, rats were intraperitoneally injected three times per week. After 24 h from the last treatment, the rats were killed under anesthesia intraperitoneally by sodium pentobarbital (100 mg/kg body weight), and then some investigations were performed. Blood was collected by cardiac puncture, then centrifuged at 4000 rpm for 15 min. Serum was stored at − 20 °C and then used in biochemical and hormonal analyses. Ovary and uterus were dissected and washed with 0.9% saline, dried on filter paper, and weighed.

2.5 Serum hormone analysis

The sera obtained from all groups ($n = 4$, from each group) were analyzed for estrogen (E2), progesterone (P4), follicle-stimulating hormone (FSH), and luteinizing hormone (LH) level by ELISA using kits from SunLong Biotech Co., Ltd. This ELISA kit uses the Sandwich-ELISA technique.

2.6 Oxidative stress investigation

For oxidative stress analysis, autopsy samples were obtained from the ovary and uterine of rats in all groups ($n = 4$, from each group) and stored at − 20 °C. A piece of each tissue was weighed and homogenized in 10 mmol/L phosphate buffer saline (PBS) as 10% (W/V) at pH 7.4. The homogenates were centrifuged, and the supernatants were used to assay malondialdehyde (MDA) according to Ohkawa et al. (1979) and total antioxidant based on the method of Koracevic et al. (2001) [19, 20].

2.7 Hematoxylin and eosin stain

The ovary and uterus of separate groups ($n = 3$, from each group) were fixed in a 10% formalin buffer solution for 24 hours for histological analysis by light microscopy. After washing with tap water, dehydration was done using serial dilutions of alcohol (methyl, ethyl, and absolute ethyl). Specimens were cleared in xylene and embedded in paraffin for 24 h at 56° in a hot air oven. Paraffin beeswax tissue blocks were sectioned at a thickness of 4 microns using a sliding microtome. For routine evaluation, the acquired tissue sections were collected on glass slides, deparaffinized, and stained with hematoxylin and eosin stain, then examined using an electric light microscope [21].

2.8 Immunohistochemistry studies for activated caspase-3

For immunohistochemistry, examinations were used caspase-3 (apoptotic marker) positive cells were determined with the streptavidin–biotin peroxidase staining method [22]. The quantitative analysis of caspase-3 was performed using ImageJ software (Version 1.53i). The DAB signal was quantified using ImageJ software to estimate the differences in immunoreactivity. Fifteen fields were selected from each group (5 fields x three rats/ group). The optical density was calculated according to the following equation: OD = log (Max. gray intensity/mean gray intensity) to determine the degree of immunoreactivity (darkness) of the stained cells by the DAB signal [23].

$$\mathrm{OD} = \log\left(\frac{\mathrm{Max}}{\mathrm{Mean}}\right).$$

2.9 Statistical analysis

Data were expressed as a mean with standard error (mean ± SEM) for each group. Statistical differences between the groups were determined using the one-way ANOVA test, followed by Tukey's multiple comparison

post hoc analysis for multiple comparisons between groups using SPSS Software. The level of statistical significance was set at $p < 0.05$.

3 Results

3.1 Characterization

3.1.1 XRD

XRD pattern appears in the fingerprint peaks position of magnetite nanoparticles according to Bruker database where magnetite nanoparticles code was COD 1011032. XRD curve is absent of any impurities or undesired chemicals with a peak equal to (2600) (Fig. 1).

The Fe_3O_4NPs pattern, as shown in Fig. 1, demonstrates the presence of five characteristic peaks for magnetite nanoparticles at $2\theta = 30°$, 36°, 43°, 57.5°and 63°.

3.1.2 TEM

TEM image confirms the nano-size of magnetite with a size of about 35 nm and a spherical shape with less aggregate, as demonstrated in Fig. 2.

3.2 Effect of magnetite nanoparticles on weight change

3.2.1 Change in body weight

There was no difference in body weight gain of animals after administration of nano-magnetite compared with the control group (Table 1).

3.2.2 Change in the absolute and relative weight of reproductive organs

There was no difference in absolute and relative weight of both reproductive organs (ovaries and uterus) after IP injection of nano-magnetite compared to controls (Table 1).

3.3 Serum hormones results

3.3.1 Estrogen and progesterone

Compared to the control group, the estrogen level was significantly decreased, while there was no change in the progesterone level after injection with nano-magnetite. However, the level of both hormones decreased significantly in a dose-dependent manner (Table 2).

3.3.2 Follicle-stimulating hormone (FSH) and luteinizing hormone (LH)

The FSH and LH concentration was significantly reduced after IP injection of nano-magnetite with a low

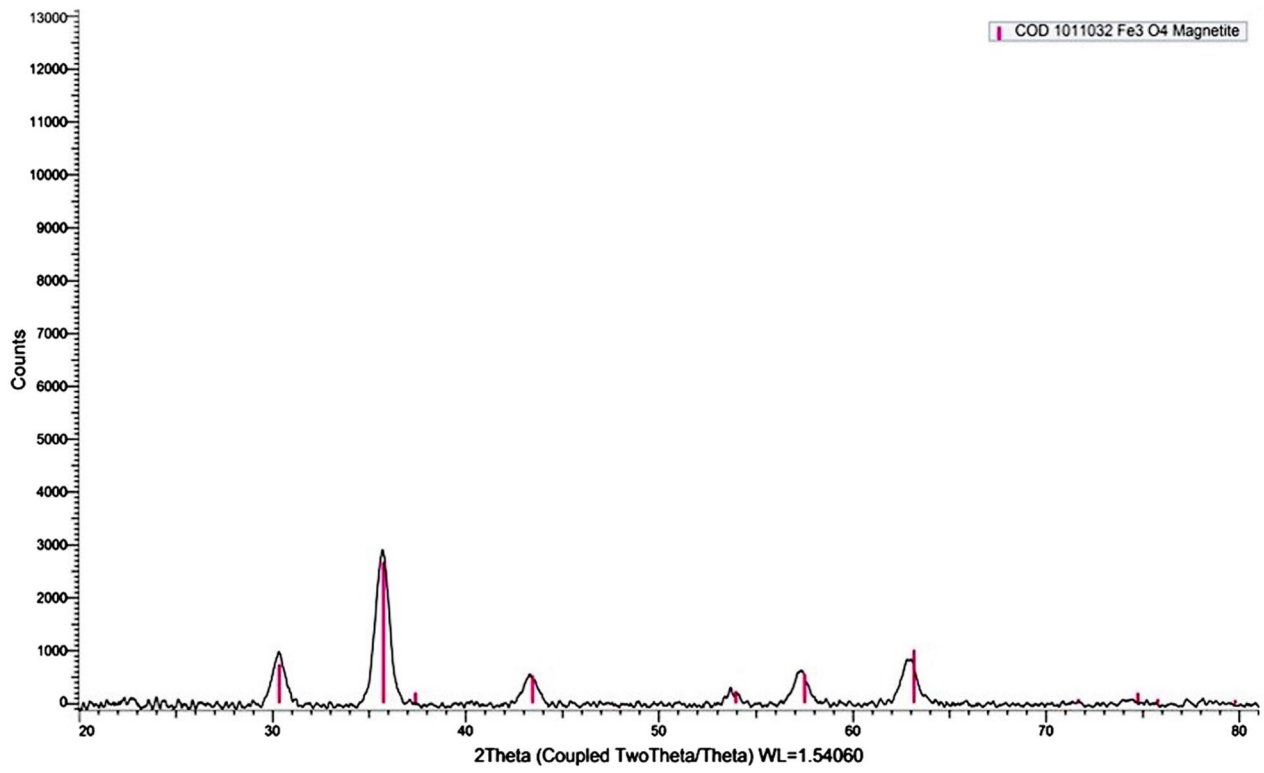

Fig.1 XRD pattern

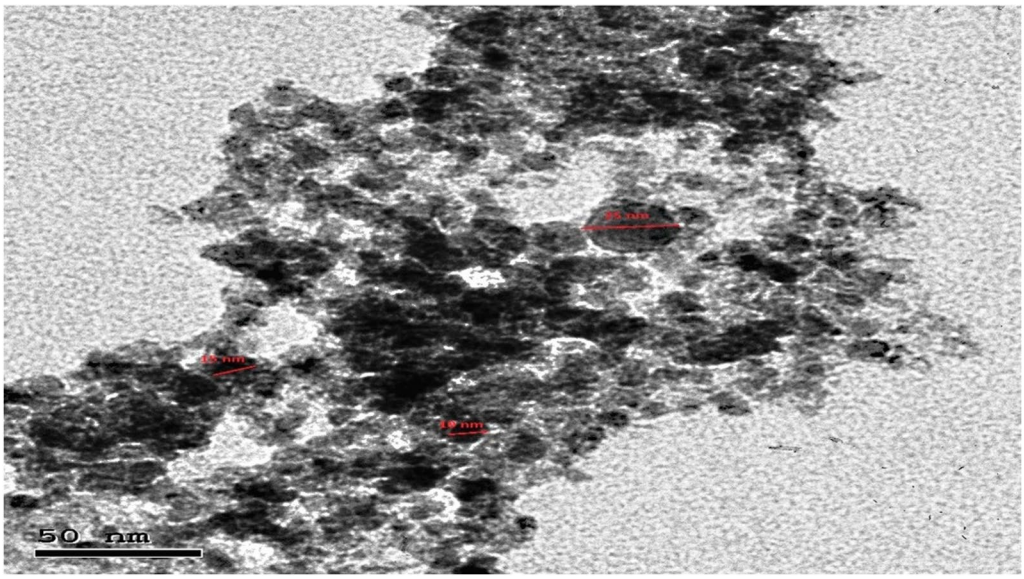

Fig. 2 TEM image conforming the nano-size of Fe_3O_4 NPs with size about 35 nm and spherical shape with aggregate less

Table 1 Effect of Fe_3O_4 NPs on body weight change and organ weight

Parameters Groups	BWC (g)	ARO (g)	RRO (%)	ALO (g)	RLO (%)	AU (g)	RU (%)
Control	17.57 ± 1.84	0.05 ± 0.00	0.02 ± 0.00	0.05 ± 0.00	0.02 ± 0.00	0.44 ± 0.07	0.21 ± 0.03
Treated 1	16.57 ± 3.42	0.16 ± 0.064	0.07 ± 0.03	0.15 ± 0.053	0.07 ± 0.02	0.50 ± 0.12	0.24 ± 0.06
Treated 2	13.00 ± 3.00	0.11 ± 0.031	0.05 ± 0.01	0.08 ± 0.013	0.04 ± 0.00	0.44 ± 0.09	0.23 ± 0.04
F value	0.71	1.8	1.9	2.6	2.7	0.12	0.09
P value	0.5	0.18	0.16	0.09	0.09	0.88	0.9

The data expressed as mean ± standard error of the mean. $N = 7$

BWC, body weight change; ARO, absolute right ovary; RRO, relative right ovary; ALO, absolute left ovary; RLO, relative left ovary; AU, absolute uterus; RU, relative uterus

Table 2 Effect of Fe_3O_4 NPs on female reproductive hormones

Parameters Groups	Estrogen (pg/ml)	Progesterone (pg/ml)	FSH IU/L	LH IU/L
Control	37.02 ± 2.89	3.625 ± 0.169	6.47 ± 0.36	6.65 ± 0.259
Treated 1	14.0 ± 3.34[a,b]	9.76 ± 3.41	1.47 ± 0.085[a,b]	1.22 ± 0.047[a,b]
Treated 2	5.50 ± 0.50[a,b]	5.10 ± 1.18	17.57 ± 0.84[a,b]	8.25 ± 0.272[a,b]
F value	40.3	3.06	238.1	282.5
P value	0.00	0.097	0.00	0.00

The data expressed as mean ± standard error of the mean

[a] $P < 0.05$ as compared with control

[b] $P < 0.05$ between treated groups

dose (5 mg/kg) compared with control, while a high dose (10 mg/kg) of nano-magnetite caused a significant elevation in FSH and LH levels compared to the control group (Table 2).

3.4 Effect of iron nanoparticles on oxidative stress markers

3.4.1 MDA and total antioxidant levels in ovary

IP injection of nano-magnetite at a high dose level induced a significant increase in ovarian MDA

Table 3 Effect of Fe_3O_4 NPs on ovarian oxidative status

Parameters Groups	MDA (nmol/ml)	TAC (mM/L)
Control	75.43 ± 14.27	0.467 ± 0.124
Treated 1	398.02 ± 81.02	0.259 ± 0.031
Treated 2	952.86 ± 249.9[a]	0.037 ± 0.009[a]
F value	8.5	8.3
P value	0.005	0.005

The data are expressed in terms of the mean and standard error of the mean

[a] $P = 0.05$ as compared with control

Table 4 Effect of Fe_3O_4 NPs on uterine oxidative status

Parameters Groups	MDA (nmol/ml)	TAC (mM/L)
Control	28.09 ± 4.25	0.179 ± 0.024
Treated 1	150.11 ± 12.75[a]	0.213 ± 0.071
Treated 2	160.30 ± 33.24[a]	0.279 ± 0.068
F value	12.6	0.75
P value	0.001	0.49

The data are presented as a mean and standard error of the mean

[a] $P = 0.05$ as compared with control

concentration and a decrease in total antioxidant activity compared with the control group. In contrast, a low nano-magnetite dose did not cause any change in MDA and TAC levels (Table 3).

3.4.2 MDA and total antioxidant levels in the uterus

Administration of nano-magnetite [low and high doses] caused a significant elevation in uterine MDA and TAC levels in comparison with the control group (Table 4).

3.5 Histopathological studies

3.5.1 Ovarian tissue

3.5.1.1 Control A thin layer of dense fibrous connective tissue called tunica albuginea covered the ovaries section from the control, surrounded by a single layer of cuboidal or flat cells (germinal epithelium); secondary follicles were also secondary observed. These follicles were formed of an oocyte surrounded by zona pellucida, corona radiate (granulosa cells immediately surrounding the oocyte), and cumulus oophorus (granulosa cells that protrude into the antrum). The third part of granulosa cells lining the follicular cavity was also present. Then the follicle was surrounded by theca folliculi. Graafian follicle, atretic follicle, and stroma were also seen (Fig. 3A).

3.5.1.2 Low dosage group The ovarian section revealed degenerative follicles with the presence of many atretic follicles. Their cells appeared apoptotic, with deep acidophilic cytoplasm and pyknotic nuclei. Some sections revealed secondary and tertiary follicles with almost lost cells of corona radiata and cumulus oophorus. Moreover, there was vacuolation in the granulosa cells of different follicles, in addition to vacuolation of the interstitial cells of stromal cells (Theca externa) with apoptotic cells having deep acidophilic cytoplasm and pyknotic nuclei. There was also a cyst, normal corpus luteum, dilated vessels in the ovarian medulla, congested blood vessels occupying the ovarian stroma, hemorrhage, and dilated vein was seen (Fig. 3B–D).

3.5.1.3 High dosage group Regarding ovarian sections of female rats treated with 0.2 ml/kg of Fe_3O_4 NPs, there were degenerative follicles with the presence of many atretic follicles. Their cells appeared apoptotic with deep acidophilic cytoplasm and pyknotic nuclei. Some sections revealed secondary follicles where the cells of zona granulosa are degenerated and disorganized. Other sections showed tertiary follicles containing antrum and completely degenerated follicles. Furthermore, degenerated and normal corpora lutea were visible. Dilated congested blood vessels, dilated veins with RBCs, and follicular cysts were also observed. Additionally, there was vacuolation and degeneration in the interstitial cells of stromal cells (Fig. 3E–I).

3.5.2 Uterine tissue

3.5.2.1 Control group Tissue sections from the uterus of female rats control group revealed normal uterine histology with normal uteri with slit-like lumina and their walls formed of inner endometrium, middle myometrium, and outer perimetrium. The endometrial lining was simple columnar epithelial cells. The underlying lamina propria contained tall endometrial glands lined with simple columnar epithelial cells with vesicular nuclei. Few apoptotic cells with pyknotic nuclei and vacuolated cytoplasm were detected in the surface epithelium, the endometrial glands, and the endometrial lamina propria. There were some mitotic figures in the epithelium. The smooth muscles of the myometrium were divided into inner circular and outer longitudinal layers with a layer of blood vessels in between. The myocytes possessed acidophilic cytoplasm and pale nuclei (Fig. 4A–C).

3.5.2.2 Low dosage group A cross section of the uterus from female rats treated with 0.1 ml/kg of Fe_3O_4 NPs showed increased folding of the lumen cavity, with many luminal columnar epithelial cells undergoing

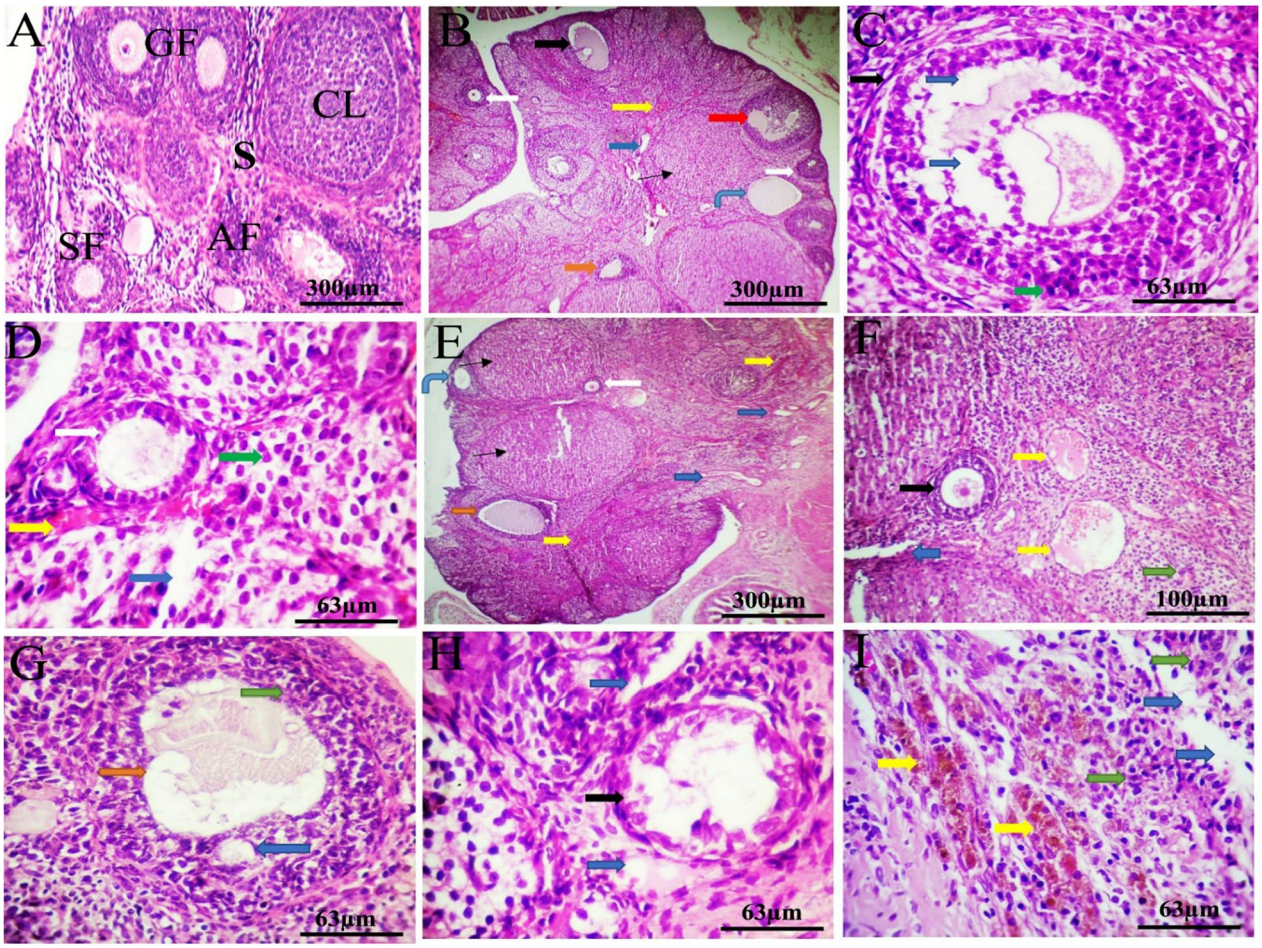

Fig. 3 Photomicrographs of an ovarian section (H&E stain, $n = 3$ from each group). Control (**A**): normal atretic follicle (AF), Graafian follicle (GF), stroma (S), corpus luteum (CL), and secondary follicles (SF). Low dose (**B**–**D**): degenerative follicles, the primary follicle (white arrow), the tertiary follicle (red arrow), degenerated secondary follicle (black arrow), vacuolation (blue arrow), cyst (curved blue arrow), corpus luteum (thin arrow), dilated vessels in the ovarian medulla and hemorrhage (yellow arrow), and atretic follicle (orange arrow), apoptotic cells having deep acidophilic cytoplasm with pyknotic nuclei (green arrow), and abnormal spaces within the stroma (vacuolation) (blue arrow). **D** Degenerated granulosa cells (blue arrows), pyknosis (green arrow), and a slight degeneration in ovarian stromal cells or theca (blue arrow). High dose (**E**–**I**): degenerated corpus luteum (thin black arrow), the primary follicle (white arrow), the atretic follicle (orange arrow), follicular cysts (bent blue arrow), congested blood vessels (yellow arrow), and vacuolation in stromal cells (blue arrow), degenerated granulosa cells (black arrow), apoptotic cells having deep acidophilic cytoplasm with pyknotic nuclei (green arrow)

hyperplasia, disaggregation, and vacuolar degeneration. The lumen cavity's epithelial cells lost their columnar shape and became flattened. The sections also demonstrated congested blood vessels in the myometrium and inflammation in the endometrium layer. Moreover, apoptosis with darkly stained pyknotic nuclei was seen in the endometrium cells and luminal epithelium. Furthermore, endometrial glands increase with many linings epithelial cells undergoing vacuolar degeneration and apoptosis (Fig. 4D–F).

3.5.2.3 High dosage group A cross section of the uterus from female rats treated with 0.2 ml/kg of Fe_3O_4 NPs revealed increased disorganization and luminal epithelium cavity folding. Moreover, apoptosis in the luminal epithelial cavity, the cells of the endometrium itself, and myometrium with many epithelial cells undergoing vacuolar degeneration. Furthermore, a high level of degeneration in cells of perimetrium and stroma was seen. It also demonstrated a high level of apoptotic cells with darkly stained pyknotic nuclei within the luminal

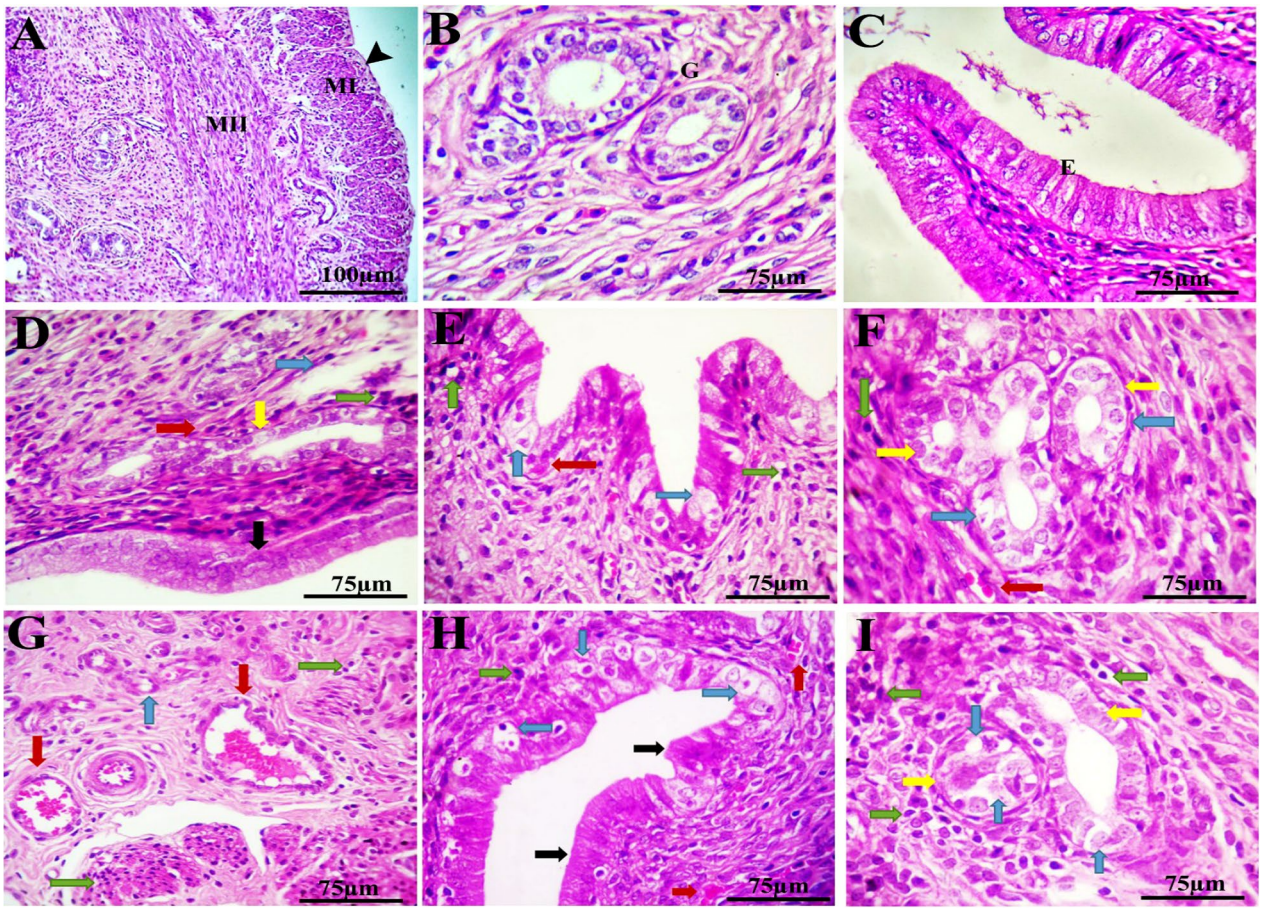

Fig. 4 Photomicrographs of a uterine section (H&E stain, $n=3$ from each group). Control (**A**–**C**): normal longitudinal muscle myometrium (MI), circular muscle myometrium (MII), endometrial gland (G), and inner endometrium (E). Low dose (**D**–**F**): degeneration of glandular epithelial cells and in the epithelial cells of endometrium itself (blue arrows), congested blood vessels in longitudinal muscle layer (red arrow), apoptotic cells with deeply stained pyknotic nuclei (green arrow), hyperplasia and disaggregation of epithelial cells of the luminal epithelium of endometrium layer (black arrow) and degeneration of endometrial glands with vacuolar degeneration (yellow arrow). High dose (**G**–**I**): high percentage of inflammation and dilated congested blood vessels (red arrow), high level of apoptotic cells with pyknotic nuclei (green arrow), vacuolar degeneration change (blue arrow). **H** Degeneration in epithelial cells of endometrium (blue arrow)

epithelium cavity and the stroma. The sections revealed endometrial glands with many lining epithelial cells undergoing vacuolar degeneration and apoptosis.

Moreover, hyperplasia of epithelial cells of the luminal epithelium of the endometrium layer was visible. The section also revealed a high percentage of inflammation and congested dilated blood vessels (Fig. 4G–I).

3.6 Morphometric outcome

NPS treatment caused an increase in various histopathological markers such as vascular congestion and cellular damage (apoptosis and/or necrosis), as shown in Table 5. There was no difference between groups in terms of average corpus luteum, preantral, antral, griffin, and atretic follicle counts (Table 6).

There was a significant decrease in the luminal diameter, endometrium thickness, and endometrial glands diameter between the treated and control groups. In addition, there was a significant decrease in the height of epithelial cells of the lumen (Table 7).

3.7 Effect of magnetite nanoparticles on immunohistochemistry for activated caspase-3

When compared to the control group, nano-magnetite injection at low and high doses caused a significant increase in immunohistochemical caspase-3 expression in both ovarian and uterine tissues (Figs. 5, 6; Table 8).

Table 5 Follicle cell degeneration, vascular congestion, hemorrhage, inflammation, and total damage scores between study groups

Parameter	Control	Low	High
Luminal diameter (μm)	15.7 ± 1.5	29.3 ± 1.6[a]	32.0 ± 1.4[a]
Myometrium thickness (μm)	39.2 ± 2.1	37.8 ± 2.2	33.9 ± 3.8
Endometrium thickness (μm)	59.8 ± 2.0	51.2 ± 2.1[a]	31.5 ± 1.4[ab]
Diameter of endometrial glands (μm)	17.6 ± 0.76	16.0 ± 0.88	14.3 ± 0.90[a]
Height of epithelial cells of lumen (μm)	8.2 ± 0.21	10.3 ± 0.50[a]	10.6 ± 0.41[a]

The data are expressed as mean ± standard error of the mean

[a] $P < 0.05$ as compared with control

[b] $P < 0.05$ between treated groups

Table 6 Number of ovarian follicles in rats exposed to Fe_3O_4 NPs

Parameter	Control	Low	High	*F* value
No. of preantral follicles	1.8 ± 0.16	0.50 ± 0.22[a]	0.30 ± 0.21[a]	16.5
No. of antral follicles	1.8 ± 0.16	0.83 ± 0.16[a]	0.83 ± 0.16[a]	12
No. of Graafian follicles	2 ± 0.00	1.1 ± 0.16[a]	0.5 ± 0.22[ab]	21.78
No. of atretic follicles	0.5 ± 0.22	1.6 ± 0.33[a]	1.8 ± 0.16[a]	4.3
No. of corpus lutea	1.1 ± 0.16	1.1 ± 0.30	1.0 ± 0.44	0.086

The data are expressed as mean ± standard error of the mean

[a] $P < 0.05$ as compared with control

[b] $P < 0.05$ between treated groups

4 Discussion

This study provides a deep insight into the impact of administered magnetite nanoparticles on the female rat reproductive system by evaluating the change in reproductive hormones, lipid peroxidation, total antioxidant capacity, and the ovarian and uterine tissues' histopathological alternation, and caspase-3 expression level. The rats were observed after 24 h from each administration. The animals did not show any sign of discomfort (lethargy, nausea, vomiting, or diarrhea) during the whole duration of the experiment.

There was no change in body weight in treated groups compared with control groups. A study has suggested that the injection of ION (Fe_3O_4 coated with dimercaptosuccinic acid) at different doses had no adverse effects on weight changes of adult mice even after three months [24]. In contrast, a study by [25] found that high-dose Fe_3O_4 NMs therapy substantially reduced the rats' body weight from week 2 to week 4. According to our findings, there are no changes in food intake between the treated groups and the control; consequently, magnetite nanoparticles may not affect the weight taken at 5 and 10 mg/kg concentration intraperitoneally for 30 days.

In our study, we have measured both relative and absolute weight of the right, left ovary, and uterus, and the results indicate that there was no change in both relative and absolute weights of both reproductive organs (ovaries & uterus) among female rats treated with a low dosage and high dosage when compared with the control group.

A study by [26] showed no significant difference between the weight of ovaries in animals receiving iron nanoparticles in different doses and animals receiving conventional iron oxide. In contrast to our findings, another study [27] found that after 30 days of therapy, animal groups subjected to greater dosages of Ag-NPs had a significant increase in body weight and ovary weight. Another study by [28] found that rats given MoO3 NPs significantly reduced right ovary and uterine weight compared to the control group, and [29] revealed a substantial decrease in the relative uterine weight coefficient after treatment with high Cu-NP dosage.

NPs can also imbalance sex female hormones, where sex hormones sustain the reproductive cycle, which is vital for the female reproductive system. The inequity of

Table 7 Uterine tissue morphometric changes between study groups

Parameter	Degree	Control	%	Low	%	High	%
Follicle cell degeneration	None	13	65	0	0	0	0
	Mild	7	25	10	50	7	25
	High	0	0	10	50	13	75
Vascular congestion	None	15	75	0	0	0	0
	Mild	5	25	13	65	12	60
	High	0	0	7	25	8	40

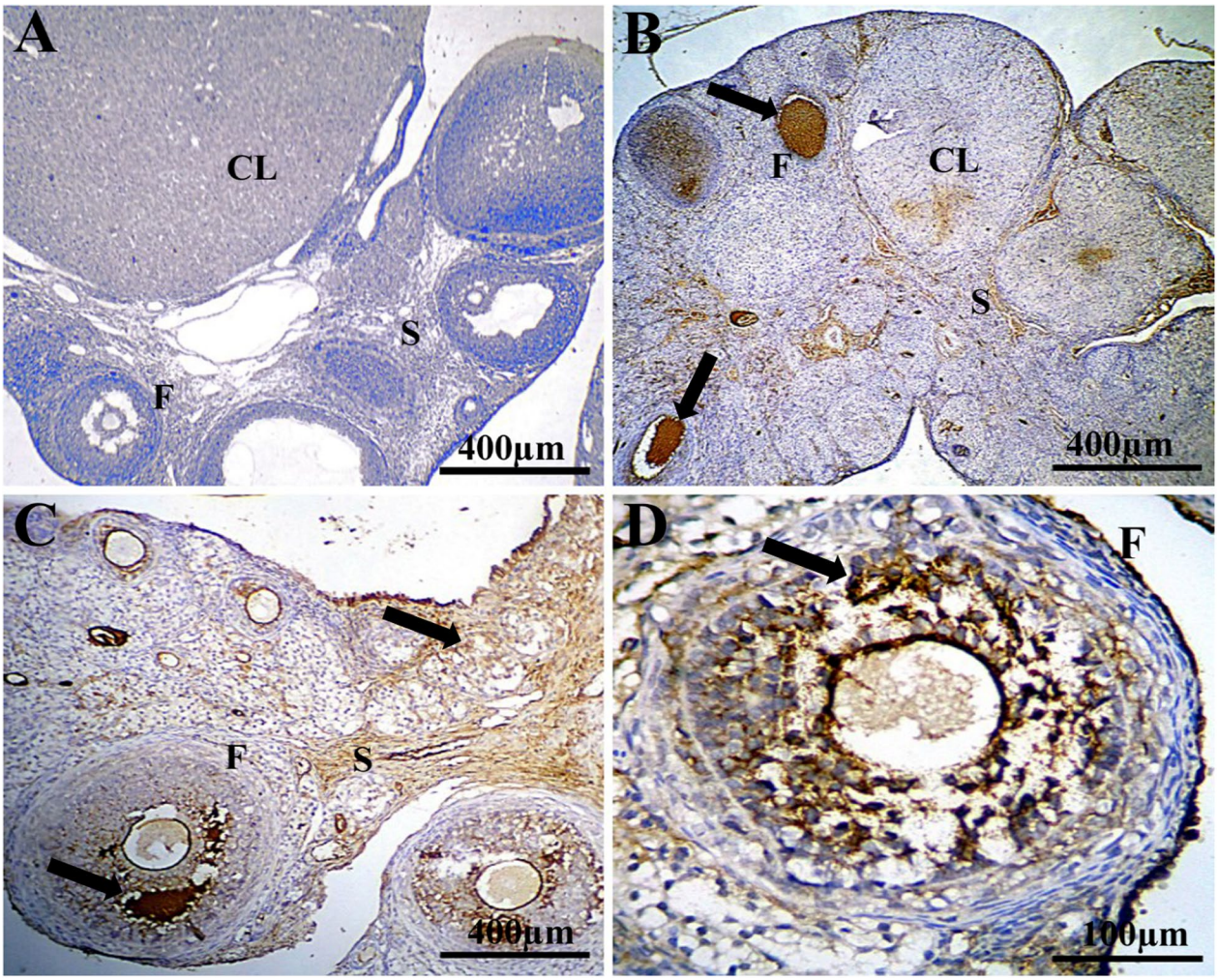

Fig. 5 Immunohistochemistry comparing caspase-3 staining in ovarian tissue ($n = 3$ from each group). Control (**A**): negative expression of immune stain caspase-3 was observed. Magnetite-treated groups (**B**–**D**): positive expressions of immune stain caspase-3 were observed (black arrows). Many follicles (F) in various stages of development, corpus luteal (CL), and stroma (S)

sex hormones generated by NPs could impact fertility [3]. The neurohormones such as GnRH, follicle-stimulating hormone (FSH), and luteinizing hormone (LH) secreted by the hypothalamus and pituitary play vital roles in positive and negative feedback regulation through oogenesis.

Progesterone activity of both female rats treated with low and high doses decreased nonsignificantly compared to the control group. A study by [10] demonstrated that TiO_2 NP exposure caused significant reductions in P4. Another previous study by [28] revealed that exposure to MoO3 NPs led to an insignificant increase in progesterone levels compared with the control groups. Furthermore, [27] found that different doses of Ag-NPs injected intraperitoneally for varied periods resulted in a nonsignificant increase in serum progesterone.

The present study results showed that the Estrogen activity of both female rats treated with both low and high doses decreased significantly compared to the control group. In contrast, FSH and LH activity of female rats treated with low dosage decreased with significant differences compared to the control group. Moreover, the FSH and LH levels of the high dosage group were substantially increased significantly compared to the control and low dose groups.

A study by [30] found that iron oxide nanoparticle treatment led to elevated serum LH levels in female mice. Another study by [31] reported that iron oxide nanoparticle treated groups in female and male rats showed a significant increase in the production of reproductive hormones (FSH, LH, and testosterone) compared to

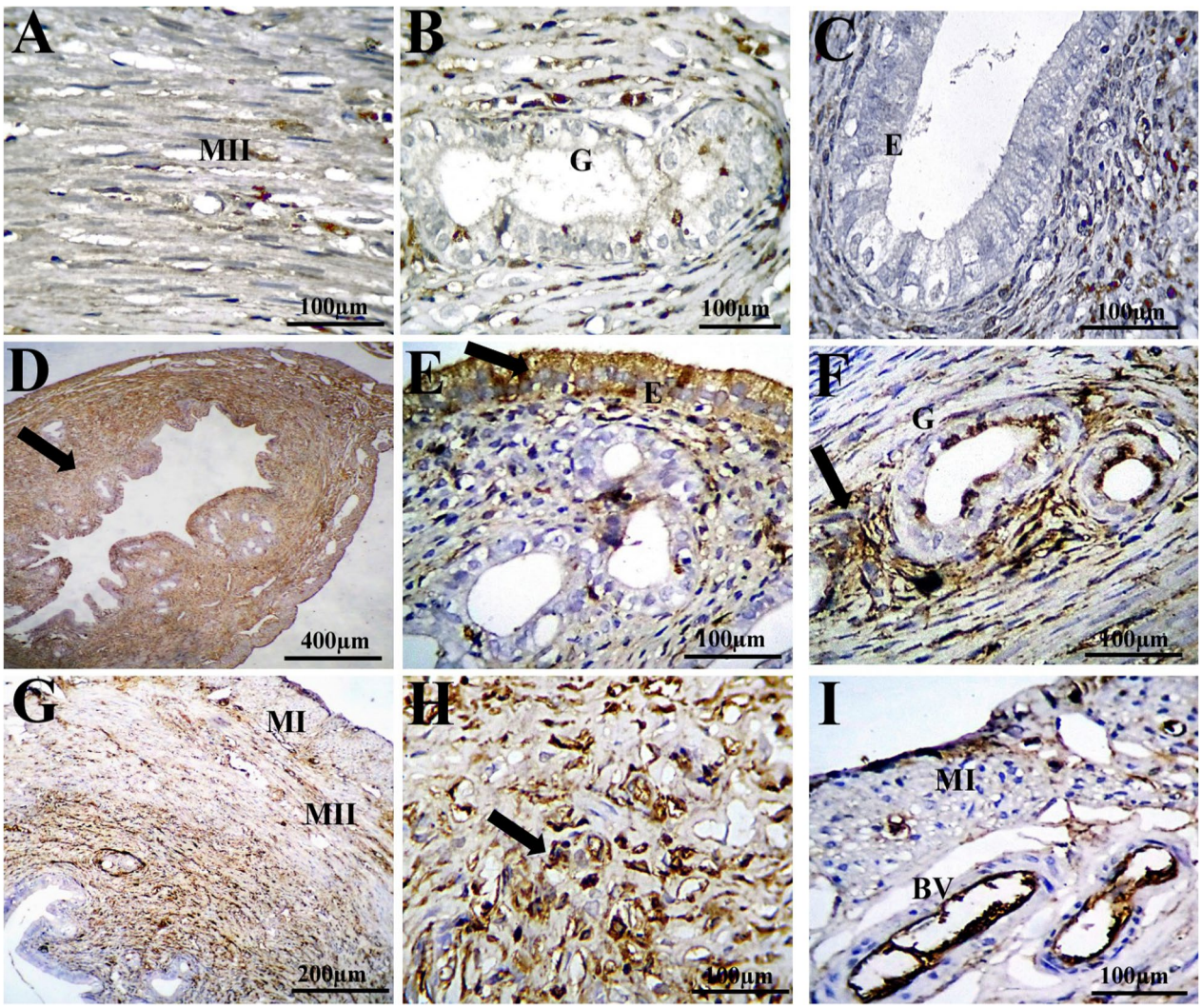

Fig. 6 Immunohistochemistry comparing caspase-3 staining in uterine tissue ($n = 3$ from each group). Control (**A**–**C**): negative expression of immune stain caspase-3 was observed. Magnetite-treated groups (**D**–**I**): positive expressions of immune stain caspase-3 were observed (black arrows). Inner endometrium (E), longitudinal muscle (LM), gland (G), and blood vessels (BV)

Table 8 Effect of Fe_3O_4 NPs on immunohistochemistry

Parameters Groups	Ovarian follicles	Ovarian stroma	Corpora luteal	Uterus
Control	0.166 ± 0.01	0.167 ± 0.004	0.186 ± 0.005	0.125 ± 0.004
Treated 1	0.249 ± 0.016[a]	0.265 ± 0.012[a]	0.293 ± 0.02[a]	0.256 ± 0.007[a]
Treated 2	0.378 ± 0.015[a]	0.318 ± 0.016[a]	0.236 ± 0.013[a]	0.337 ± 0.012[a]
F value	48.1	22.2	14.4	107.5
P value	0.00	0.00	0.00	0.00

The data are expressed as mean ± standard error of the mean

[a] $P < 0.05$ as compared with control

[b] $P < 0.05$ between treated groups

controls. Another study by [28] found that exposure to MoO3 NPs resulted in a substantial decline in estrogen levels while significantly increasing FSH and LH levels. The same results were observed by [32], suggesting that animals treated with different doses of AuNPs significantly increased LH and FSH levels.

The variation in estrogen levels found in our study could be attributed to the direct effect of nanoparticles on the ovaries, which slowed follicular growth and decreased estrogen; or interference with follicle function. Therefore, the number of estrogen-secreting follicles dropped, and estrogen secretion decreased [33, 34]. This imbalance in normal sex hormone levels could be caused by NPs' potential effect on mitochondria of functioning cells, resulting in a reduction in secretory activity. Furthermore, NPs have proven to cause oxidative stress and increase the release of reactive oxygen species (ROS), which promotes the oxidation of cellular macromolecules like proteins [35].

Massive generation of ROS is thought to be a potential mechanism for the onset and progression of toxicity injuries [36]. ROS are produced by macrophages, neutrophils, and granulosa cells in Graafian follicles, and antioxidants contribute to alleviating these effects. An imbalance between pro-oxidants and antioxidants has been proposed to cause female infertility based on its putative effects on ovulation, fertilization, embryo development, and implantation [37]. Excessive levels of ROS can quickly oxidize polyunsaturated fatty acids in ovarian follicles, resulting in lipid peroxidation. Malondialdehyde (MDA), a hazardous byproduct of lipid peroxidation that harms biological macromolecules in oocytes and granulosa cells, can induce irregular oocyte development by damaging biological macromolecules in oocytes and granulosa cells [38].

The ovarian and uterine MDA levels of female rats treated with a high dosage were increased significantly compared to the control group. Moreover, the uterine MDA level of female rats treated with a low dosage increased significantly compared to the control group. Additionally, ovarian TAC level from high dosage was significantly decreased compared to controls. In contrast, the uterine TAC level of female rats treated with low and high dosages was increased significantly compared to the control group.

Total antioxidants affect the solubility of endogenous and exogenous harmful chemicals; therefore, the substantial reduction in total antioxidants in the ovary in the current study might be related to their consumption in protecting cells from the free radicals produced. The ovary's protective system appears to have failed, as evidenced by a substantial increase in MDA levels in the ovary. However, increased total antioxidant activity (TAC) in the uterus is insufficient to detoxify the excess lipid peroxidation caused by elevated MDA levels.

Fe_3O_4 NMs dramatically increased ROS formation, resulting in cell damage and death in macrophage and lung epithelial cells, according to [39, 40]. In addition, animals receiving Fe_3O_4 NMs intraperitoneally for one week had severe oxidative stress in the liver and kidney [18]. Furthermore, after subacute IONP treatment, rats developed oxidative stress in major organs, according to [41]. On the contrary, [42] found that uncoated Fe_3O_4 NMs did not cause oxidative DNA damage or genotoxicity in human lymphoblastoid cells. Also, a study by [43] showed that acute inhalation exposure of Fe_3O_4 NPs induced a significant increase in MDA concentrations in the lungs of exposed animals compared with controls, indicating the induction of lipid peroxidation by these particles.

In the previous work by [29], rats exposed to large dosages of Cu-NPs showed signs of uterine injury, including increased MDA expression and decreased SOD expression. These findings revealed that NPs cause oxidative stress and lipid peroxidation in the uterus of rats. Also, MDA levels were considerably raised in MgO NP-treated rats' serum and tissue homogenates after 24 h and 72 h sampling intervals at 1000 mg/kg bw in research by [44], suggesting that NPs may have promoted free radical production. These free radicals rapidly target polyunsaturated fatty acids, destroying membrane lipids and releasing MDA, which is especially harmful to the viability of cells and tissues [45].

Sections of the ovary of female rats treated with Fe_3O_4Nps showed degenerative follicles with the presence of many atretic follicles. Their cells appeared apoptotic with deep acidophilic cytoplasm and pyknotic nuclei. Moreover, there was vacuolation in the granulosa cells of different follicles.

As a result, these findings matched those of a recent study that found light microscopic alterations in the ovarian tissue in female rats injected IP with ZnO NPs. In moderate and high doses, the ovarian section treated with ZnO NPs showed hyperemia, increased the corpus luteum, inflammatory cells infiltration, and fibrosis, follicular cysts [46]. Arsenic-induced lesions in the ovary and uterus and reduced folliculogenesis have been observed in research by Mehta and colleagues [47]. Furthermore, a study by [48] found that rats given high-dose Cu-NPs demonstrated significant ovarian histopathological changes, including ovarian atrophy, disruption of follicular growth, follicular atresia, and a reduction in mature follicles compared to the control group. In addition, light microscopy examinations of the ovary of all experimental groups of silver nanoparticles revealed clogged blood vessels in the stroma with

inflammatory mononuclear cell infiltration, according to research by [49].

A cross section of the uterus from female rats treated with Fe_3O_4Nps showed increased endometrium folding, with several luminal columnar epithelial cells undergoing hyperplasia, vacuolar degeneration, congested blood vessels, inflammatory cells invasion, and darkly stained pyknotic nuclei were seen.

A previous study by [50] reported that Adult female offspring of mice exposed to 100 mg/kg iron oxide NPs in utero demonstrated a substantial increase in endometrial thickness (endometrial hyperplasia), with an increased preference toward pseudostratified columnar epithelium (as opposed to typical simple columnar) when compared to the control.

A study by [51] reported that Adult female rats fed the basal diet with three doses of magnetite NPs caused histopathological changes in the kidney, spleen, liver, and lung. According to a study by [52], Fe_3O_4 nanoparticles at an LD50 level of 163.60 mg/kg also caused denaturation and necrosis in the cardiac muscles of mice. Moreover, a study by [53] showed that the histological examinations of female Wistar rats, when orally administered 10 mg/kg of α-Fe_2O_3 NPs, revealed variable organ damage at the cellular and extracellular levels. These findings also align with those of a recent study, [29] which found that intraperitoneal treatment of 12.5 mg/kg/day Cu-NPs for 14 days caused inflammatory cell infiltration, disrupted epithelial cell organization, mitochondrial enlargement, vacuolization, shortening, and reduction in microvilli on endometrial epithelial cells in the uterine tissue. In another study, female rats injected with ZnO NPs in the uterus showed minor microscopic changes [46].

Compared to the control group, the number of follicles in magnetite NPs treated groups was significantly reduced. The lower total number of follicles may indicate ovarian dysfunction and raise the chance of later life reproductive capability reduction [54]. The significant apoptosis and increased incidence of atretic follicles observed in ovarian tissue could be due to diminished gonadotropins combined with lower E2 [55]. Estrogen is mandatory for follicular growth and differentiation as well as apoptosis inhibition in preantral and early antral follicles [56].

According to our findings, the height of the uterine luminal epithelial cells is increased by magnetite NPs injection. Previous research has discovered a decline in estrogen levels in rats, reducing ovarian follicle ability to reach the developmental stage required for reproductive success and altering estrogen production, which has a variety of biological impacts throughout the body. However, the elevation in luminal epithelium height happened physiologically due to estrogen's action on uterine tissue, which caused an increase in cell proliferation and size and stimulated uterine growth [57].

Magnetite NPs caused tissue deterioration in the uterus. Since uterine growth is predominantly dependent on estradiol, the degenerative alterations could be ascribed to negative consequences caused by reduced blood estradiol levels. Due to the insufficient estrogen, the ordinary uterine structure was disrupted, resulting in the degradation of luminal epithelial cells and endometrial glands [58].

As mentioned before, the Fe_3O_4NPs administration increased the level of lipid peroxidation and oxidative stress by increasing the ROS level, decreasing the level of total antioxidants, and increasing the MDA level. Consequently, ROS accumulation enhanced apoptosis by collapsing the mitochondrial potential, initiating the mitochondrial oxidation channel, and releasing cytochrome C from mitochondria to the cytosol [59].

Apoptosis is the form of cell death frequent during follicular atresia and luteal regression and is typically associated with the activation of caspases [60]. Extrinsic (i.e., mitochondria-independent) apoptosis and mitochondria-induced intrinsic apoptosis are the two most common ways to trigger apoptosis [61]. The binding of pro-apoptotic ligands facilitates extrinsic apoptosis to cell surface receptors, which activates the downstream effector caspase-8. Caspase-8 and caspase-3 can be cleaved by activated caspase-8, resulting in cell death. In contrast, Cytochrome c is involved in the intrinsic or mitochondrial apoptotic process, which is triggered by the release of cytochrome c from the outer mitochondrial membrane into the cytoplasm. Cytochrome c interacts with apoptosis activating factor 1 (Apaf-1) and activates caspase-9, subsequently activating executor caspase-3 [29].

Caspase-3 is a cysteine aspartic acid protease (caspase) that belongs to the caspase family. Caspase activation in a sequential manner is essential for cell apoptosis [49].

Caspase-3 expression in ovarian follicles, ovarian stroma, corpora lutea, and uterine tissue of female rats treated with low and high doses was increased significantly compared to the control group.

These findings agree with a study by [49] that indicated that exposure to Ag-NPs given orally causes a positive reaction for caspase-3, which is an indicator of the presence of apoptosis. These favorable ovarian tissue responses increased in dosage and duration-dependent manner. Another study by [29] found that different doses of Cu-NPs significantly increased the expression levels of caspase-8, caspase-3, and caspase-9 proteins in the ovaries compared to the control.

Our findings matched research by [29], which found that Cu-NPs might trigger apoptosis in uterine tissues by stimulating the release of cytochrome c into

the cytoplasm, thereby activating the expression of caspase-3, caspase-8, and caspase-9 in comparison with the control group. In addition, a 90-day oral toxicity study in female mice at a dose of 10 mg/kg bw revealed that TiO_2 nanoparticles concentrate in the ovaries, causing ovarian damage, oxidative stress, mineral element distribution, and sex hormone imbalance, as well as a reduction in fertility and conception rate [10, 62].

5 Conclusion

Based on the study findings, the P administration of Fe_3O_4NPs can negatively affect sexual hormones (FSH, LH, E2, and P4), causing a deleterious impact on the uterus and ovary histology. Consequently, reactive oxygen species accumulation had the potential to enhance apoptosis by increasing caspase-3 expression, resulting in a negative impact on reproductive health. Future studies of Fe_3O_4NPs exposure to women's health will be based on these findings.

5.1 Limitations

Our study has some limitations as measuring total antioxidant capacity and MDA only as an indicator of oxidative stress investigation. It would have been more accurate if we had measured some antioxidant enzymes such as catalase, glutathione reductase, glutathione peroxidase, and superoxide dismutase.

5.2 Future directions

Further studies are needed to investigate the mechanism of action of magnetite nanoparticles on the female reproductive system and target and investigate signal pathways of some specific genes associated with ovarian failure, follicular atresia, and abnormal follicular development.

Abbreviations

ION Nps: Iron oxide nanoparticles; Fe_3O_4: Magnetite; E2: Estrogen hormone; P4: Progesterone hormone; LH: Luteinizing hormones; FSH: Follicle-stimulating hormones; MDA: Malondialdehyde; TAC: Total antioxidant; IP: Intraperitoneally; NMs: Nanomaterials; MRI: Magnetic resonance imaging; XRD: X-ray diffraction; TEM: Transmission electron microscopy; GnRH: Gonadotropin-releasing hormone; SOD: Superoxide dismutase; GSH: Glutathione reduced.

Acknowledgements

We would like to express special thanks to all staff members of the Zoology Department at Cairo University/Faculty of Science for their help to accomplish the laboratory work in the study.

Author contributions

All authors read and approved the final manuscript.

Funding

This research received no external funding.

Availability of data and materials

The datasets used and/or analyzed during the current study are available from the corresponding author on reasonable request.

Declarations

Ethics approval and consent to participate

The protocol of the study was set up by the international law on the protection of animals in the laboratory and Ethical approval for animal use was obtained from Institutional Animal Care and Use Committee (CU-IACUC) Cairo-University (CUFS/Comp&Emb/CU/I/F/74/19).

Consent for publication

Not applicable.

Competing interests

The authors declare no conflict of interest.

Author details

[1]Department of Chemistry, Biotechnology, Faculty of Science, Cairo University, Giza, Egypt. [2]Department of Zoology, Faculty of Science, Cairo University, Giza, Egypt. [3]Department of Chemistry, Faculty of Science, Cairo University, Giza, Egypt.

Received: 21 December 2021 Accepted: 19 July 2022
Published online: 29 July 2022

References

1. Ema M et al (2017) A review of reproductive and developmental toxicity of silver nanoparticles in laboratory animals. Reprod Toxicol 67:149–164
2. McAuliffe ME, Perry MJ (2007) Are nanoparticles potential male reproductive toxicants. A literature review. Nanotoxicology 1(3):204–210
3. Wang R, Song B, Wu J, Zhang Y, Chen A, Shao L (2018) Potential adverse effects of nanoparticles on the reproductive system. Int J Nanomed 13:8487–8506
4. Ghazanfari MR, Kashefi M, Shams SF, Jaafari MR (2016) Perspective of Fe3O4 nanoparticles role in biomedical applications. Biochem Res Int 2016:32
5. Blaney L. Magnetite (Fe_3O_4): properties, synthesis, and applications.
6. Lankveld DPK, Oomen AG, Krystek P, Neigh A, Troost-de Jong A, Noorlander CW, De Jong WH (2010) The kinetics of the tissue distribution of silver nanoparticles of different sizes. Biomaterials 31(32):8350–8361. https://doi.org/10.1016/j.biomaterials.2010.07.045
7. Balasubramanian SK, Jittiwat J, Manikandan J, Ong C-N, Yu LE, Ong W-Y (2010) Biodistribution of gold nanoparticles and gene expression changes in the liver and spleen after intravenous administration in rats. Biomaterials 31(8):2034–2042. https://doi.org/10.1016/j.biomaterials.2009.11.079
8. Wu T, Tang M (2018) Review of the effects of manufactured nanoparticles on mammalian target organs. J Appl Toxicol 38(1):25–40
9. Kim JS, Yoon TJ, Yu KN et al (2006) Toxicity and tissue distribution of magnetic nanoparticles in mice. Toxicol Sci 89(1):338–347
10. Gao G, Ze Y, Li B, Zhao X, Zhang T, Sheng L et al (2012) Ovarian dysfunction and gene-expressed characteristics of female mice caused by long-term exposure to titanium dioxide nanoparticles. J Hazard Mater 243:19–27
11. Kong L, Tang M, Zhang T et al (2014) Nickel nanoparticles exposure and reproductive toxicity in healthy adult rats. Int J Mol Sci 15(11):21253–21269
12. Liu J, Zhao Y, Ge W et al (2017) Oocyte exposure to ZnO nanoparticles inhibits early embryonic development through the γ-H2AX and NF-κB signaling pathways. Oncotarget 8(26):42673–42692
13. Cooper TG, Noonan E, Von Eckardstein S, Auger J, Baker HW, Behre HM, Haugen TB, Kruger T, Wang C, Mbizvo MT, Vogelsong KM (2010) World Health Organization reference values for human semen characteristics. Hum Reprod Update 16(3):231–245

14. Olooto WE, Amballi AA, Banjo TA (2012) A review of female Infertility; important etiological factors and management. Microbiol Biotech Res 2(3):379
15. Noori A, Amiri G (2011) Effect of magnetic iron oxide nanoparticle on pregnancy and testicular development of mice. Clin Biochem. 44(13):S324
16. Mahmoudi M, Laurent S, Shokrgozar MA, Hosseinkhani M (2011) Toxicity evaluations of superparamagnetic iron oxide nanoparticles: cell "vision" versus physicochemical properties of nanoparticles. ACS Nano 5(9):7263–76
17. El Ghandoor H, Zidan HM, Khalil MM, Ismail MI (2012) Synthesis and some physical properties of magnetite (Fe_3O_4) nanoparticles. Int J Electrochem Sci 7(6):5734–5745
18. Ma P, Luo Q, Chen J, Gan Y, Du J, Ding S et al (2012) Intraperitoneal injection of magnetic Fe3O4-nanoparticle induces hepatic and renal tissue injury via oxidative stress in mice. Int J Nanomed 7:4809–4818
19 Kei S (1978) Serum lipid peroxide in cerebrovascular disorders determined by a new colorimetric method. Clin Chim Acta. 90(1):37–43
20 Koracevic D, Koracevic G, Djordjevic V, Andrejevic S, Cosic V (2001) Method for the measurement of antioxidant activity in human fluids. J Clin Pathol. 54(5):356–614
21 Kiernan JA, Horobin RW (2009) special issue devoted to hematoxylin, hematein, and hemalum. Biotech Histochem. 2009:1–2
22. Sternberger LA (1986) Immunocytochemistry, 3rd edn. Churchill Livingstone, London
23. Abd-Elhafeez HH, Soliman SA, Attaai AH, Abdel-Hakeem SS, El-Sayed AM, Abou-Elhamd AS (2021) Endocrine, stemness, proliferative, and proteolytic properties of alarm cells in ruby-red-fin shark (Rainbow Shark), Epalzeorhynchos frenatum (Teleostei: Cyprinidae). Microsc Microanal 27(5):1251–1264
24. Noori A, Parivar K, Modaresi M, Messripour M, Yousefi MH, Amiri GR (2011) Effect of magnetic iron oxide nanoparticles on pregnancy and testicular development of mice. Afr J Biotechnol 10:1221–1227
25. Reddy UA, Prabhakar PV, Mahboob M (2018) Comparative study of nano and bulk Fe_3O_4 induced oxidative stress in Wistar rats. Biomarkers 23(5):425–434
26. Poormoosavi SM, Morovvati H, Najafzadeh Varzi H, Behmanesh MA, Shahryari A, Mohamadian B (2018) Accumulation of iron oxide nanoparticle and conventional iron oxide in rat ovary and oxidative stress caused by it. Iran Red Crescent Med J. https://doi.org/10.5812/ircmj.58738
27. Qassim HA, Luaibi N. Study of the hormonal and histological effects of silver nanoparticles on thyroid, ovary and mammary glands in female rats. Reasearch; 2017. 118.
28. Asadi F, Sadeghzadeh M, Jalilvand A, Nedaei K, Asadi Y, Heidari A et al (2019) Effect of molybdenum trioxide nanoparticles on ovary function in female rats. Majallahi Ilmi Pizhuhishii Danishgahi Ulumi Pizishki Khadamati Bihdashtii Darmanii Zanjan 27(121):48–53
29. Hu S, Yang J, Rao M, Wang Y, Zhou F, Cheng G et al (2019) Copper nanoparticle-induced uterine injury in female rats. Environ Toxicol 34(3):252–261
30. Ibraheem SR, Ibrahim MR (2017) Physiological and histological effects of (zinc and iron) oxide nanoparticles on some fertility parameters in female mice. Al-Mustansiriyah J Sci 27(5):1
31. Kamel RH, AL-Taee AA. (2020) Effect of iron oxide nanopartical on the FSH, LH and testesteron hormones in the offspring of albino rats. Indian J Foren Med Toxicol 14(1):1024
32. Behnammorshedi M, Nazem H, Saleh-moghadam M (2015) The effect of gold nanoparticle on luteinizing hormone, follicle stimulating hormone, testosterone and testis in male rat. Biomed Res J. 26(2):348–352
33. Asadi F, Fazelipour S, Abbasi RH, Jahangirirad M, Tootian Z, Nedaei K et al (2017) Assessment of ovarian follicles and serum reproductive hormones in molybdenum trioxide nanoparticles treated rats. Int J Morphol 35(4):1473
34 Assadi F, Amirmoghaddami H, Shamseddin M, Nedaeei K, Heidari A et al (2016) Effect of molybdenum trioxide nanoparticles (MoO_3 NPs) on thyroid hormones in female rats. J Hum Environ Health Promot. 1(4):189–95
35. Carlson C, Hussain SM, Schrand AM, Braydich-Stolle LK, Hess KL, Jones RL et al (2008) Unique cellular interaction of silver nanoparticles: size-dependent generation of reactive oxygen species. J Phys Chem B 112(43):13608–13619
36. Barillet S, Jugan M-L, Laye M, Leconte Y, Herlin-Boime N, Reynaud C et al (2010) In vitro evaluation of SiC nanoparticles impact on A549 pulmonary cells: cyto-, genotoxicity and oxidative stress. Toxicol Lett 198(3):324–330
37. Agarwal A, Gupta S, Sekhon L, Shah R (2008) Redox considerations in female reproductive function and assisted reproduction: from molecular mechanisms to health implications. Antioxid Redox Signal 10(8):1375–1403
38. Prasad S, Tiwari M, Pandey AN, Shrivastav TG, Chaube SK (2016) Impact of stress on oocyte quality and reproductive outcome. J Biomed Sci 23(1):36
39. Naqvi S, Samim M, Abdin M, Ahmed FJ, Maitra A, Prashant C et al (2010) Concentration-dependent toxicity of iron oxide nanoparticles mediated by increased oxidative stress. Int J Nanomed 5:983–989
40. Ramesh V, Ravichandran P, Copeland CL, Gopikrishnan R, Biradar S, Goornavar V et al (2012) Magnetite induces oxidative stress and apoptosis in lung epithelial cells. Mol Cell Biochem 363(1–2):225–234
41. Reddy UA, Prabhakar PV, Mahboob M (2017) Biomarkers of oxidative stress for in vivo assessment of toxicological effects of iron oxide nanoparticles. Saudi J Biol Sci 24(6):1172–1180
42. Singh N, Jenkins GJS, Nelson BC, Marquis BJ, Maffeis TGG, Brown AP et al (2012) The role of iron redox state in the genotoxicity of ultrafine superparamagnetic iron oxide nanoparticles. Biomaterials 33(1):163–170
43. Srinivas A, Rao PJ, Selvam G, Goparaju A, Murthy PB, Reddy PN (2012) Oxidative stress and inflammatory responses of rat following acute inhalation exposure to iron oxide nanoparticles. Hum Exp Toxicol 31(11):1113–1131
44. Mangalampalli B, Dumala N, Grover P (2017) Acute oral toxicity study of magnesium oxide nanoparticles and microparticles in female albino Wistar rats. Regul Toxicol Pharmacol 90:170–184
45. Mylonas C, Kouretas D (1999) Lipid peroxidation and tissue damage. In Vivo 13(3):295–309
46. Hosseini SM, Moshrefi AH, Amani R, Razavimehr SV, Aghajanikhah MH, Sokouti Z et al (2019) Subchronic effects of different doses of Zinc oxide nanoparticle on reproductive organs of female rats: an experimental study. Int J Reprod BioMed 17(2):107
47. Mehta M, Hundal SS (2016) Effect of sodium arsenite on reproductive organs of female Wistar rats. Arch Environ Occup Health 71(1):16–25
48. Yang J, Hu S, Rao M, Hu L, Lei H, Wu Y et al (2017) Copper nanoparticle-induced ovarian injury, follicular atresia, apoptosis, and gene expression alterations in female rats. Int J Nanomed 12:5959–5971
49. Elnoury MAH, Azmy OM, Elshal AOI, Mohamed A, Ragab H, Elsherbini ESAM (2013) Study of the effects of silver nanoparticles exposure on the ovary of rats. Life Sci J 10(2):1887–1894
50. Di Bona KR, Xu Y, Gray M, Fair D, Hayles H, Milad L et al (2015) Short-and long-term effects of prenatal exposure to iron oxide nanoparticles: influence of surface charge and dose on developmental and reproductive toxicity. Int J Mol Sci 16(12):30251–30268
51. Elsayed HH, Al-Sherbini ASAM, Abd-Elhady EE, Ahmed KAEA (2014) Treatment of anemia progression via magnetite and folate nanoparticles in vivo. ISRN Nanotechnol 2014:1–13
52. Zhao S, Lin X, Zhang L, Sun L, Li J, Yang W et al (2012) The in vivo investigation of Fe_3O_4-Nanoparticles Acute Toxicity In Mice. Biomed Eng (Singapore) 24(03):229–235
53. Smital K, Niharika S, Mansee T (2020) Sub-acute toxicity assessment of green synthesized hematite nanoparticles (α-Fe_2O_3 NPs) using Wistar rat. Res J Biotechnol 15:4
54. Cansu A, Giray SG, Serdaroglu A, Erdogan D, Coskun ZK, Korucuoglu U, Biri AA (2008) Effects of chronic treatment with valproate and oxcarbazepine on ovarian folliculogenesis in rats. Epilepsia 49(7):1192–1201
55. Sato J, Nasu M, Tsuchitani M (2016) Comparative histopathology of the estrous or menstrual cycle in laboratory animals. J Toxicol Pathol [Internet] 29(3):155–162
56. Mostafapour S, Zare S, Sadrkhanlou RA, Ahmadi A, Razi M (2014) Sulpiride-induced hyperprolactinemia in mature female rats: evidence for alterations in the reproductive system, pituitary and ovarian hormones. Int J Fertil Steril 8(2):193–206
57. Alchalabi AS, Rahim H, Aklilu E, Al-Sultan II, Malek MF, Ronald SH, Khan MA (2016) Histopathological changes associated with oxidative stress induced by electromagnetic waves in rats' ovarian and uterine tissues. Asian Pac J Reprod 5(4):301–310
58. Chatterjee A, Chatterji U (2010) Arsenic abrogates the estrogen-signaling pathway in the rat uterus. Reprod Biol Endocrinol 8(1):1–11

59. Zhao X, Xiang H, Bai X, Fei N, Huang Y, Song X et al (2016) Porcine parvovirus infection activates mitochondria-mediated apoptotic signaling pathway by inducing ROS accumulation. Virol J 13(1):26
60. Abhari SMF, Khanbabaei R, Roodbari NH, Parivar K, Yaghmaei P (2020) Curcumin-loaded super-paramagnetic iron oxide nanoparticle affects on apoptotic factors expression and histological changes in a prepubertal mouse model of polycystic ovary syndrome-induced by dehydroepiandrosterone-A molecular and stereological study. Life Sci 249:117515
61. Movassagh M, Foo RS-Y (2008) Simplified apoptotic cascades. Heart Fail Rev 13(2):111–119
62. Zhao X, Ze Y, Gao G, Sang X, Li B, Gui S et al (2013) Nanosized TiO_2-induced reproductive system dysfunction and its mechanism in female mice. PLoS ONE 8(4):e59378

Publisher's Note